Pergamon

Int. J. Solids Structures Vol. 33, No. 24, pp. 3601–3610, 1996

0020-7683/96 $15.00 + .00

0020-7683(95)00201-4

EFFECT OF LOADING FREQUENCY ON FATIGUE CRACK GROWTH UNDER HIGH TEMPERATURE

ZHIXIONG QIAN, SHIGEO TAKEZONO and KATSUMI TAO
Department of Mechanical Engineering, Toyohashi University of Technology, Tempaku-cho, Toyohashi 441, Japan

(*Received* 30 *November* 1994; *in revised form* 18 *August* 1995)

Abstract—The effect of loading frequency on the fatigue crack growth under high temperature is studied. The high temperature fatigue crack growth tests for pure titanium (99.5%) are carried out under three loading frequencies (2, 6, 20 Hz). An elasto/viscoplastic constitutive equation which fully couples strain to continuum damage is used to analyse fatigue crack growth at high temperature. A damage criterion is employed for predicting the crack growth which is related to the actual material failure ahead of the crack tip. By means of FEM, the mechanical fields (σ_{ij}, ε_{ij}, D) and the dependence of crack growth rate on loading frequency and viscoplastic strain at the crack tip are investigated in detail. The numerical simulation results of the fatigue crack growth are shown and compared with the experimental ones.

The results in the present study show that: (1) the stress at the crack tip element decreases rapidly with the cyclic numbers. There is no stable state of stress distribution in the fatigue process when material damage is taken into account. (2) The crack tip stress is lower than the peak stress and the peak stress takes place at a location away from the crack tip. No stress singularity is present at the crack tip. (3) The fatigue growth rate dl/dN is closely related to the $\Delta\varepsilon_1^{vp}$ obtained by numerical analysis. If dl/dN is plotted against $\Delta\varepsilon_1^{vp}$, the relation can be expressed by a straight line in logarithmic coordinates for any loading frequency. Copyright © 1996 Elsevier Science Ltd.

1. INTRODUCTION

High temperature fatigue failure is an important cause of component failure in many industrial applications. A number of approaches, such as, J-integral, C*-integral, etc., have been proposed. These methods are an extension of conventional fracture mechanics concepts, and do not include the inherent physical mechanism of material deterioration in fatigue process (Chaboche and Bathias, 1986; Chen and Hsu, 1991). Another shortcoming of these methods is that they cannot incorporate the loading histories and the effect of the stress redistribution caused by the evolution of material damage. On the other hand, continuum damage mechanics (CDM) centered on micro defect development provides a better understanding of the fracture mechanism in structures by means of a damage variable (Lemaitre and Chaboche, 1990). Recently, CDM has been playing significant roles in analysing the characteristics of material damage and fracture. In these rules, however, the effect of loading frequency on the crack growth has been ignored except for the case of consideration of atmospheric or environmental effects. In fact, some materials, such as titanium, show the dependence of loading frequency on the fatigue crack growth even at room temperature. It is important to make clear this effect from a view of evaluation of fatigue damage.

In the present study, the effect of loading frequency on the fatigue crack growth under high temperature is investigated in detail. The high temperature fatigue crack growth tests for pure titanium (99.5%) are carried out under three loading frequencies (2Hz, 6Hz, 20Hz). An elasto/viscoplastic constitutive equation which fully couples strain to continuum damage is used to analyse fatigue crack growth at high temperature. A damage criterion is employed for predicting the crack growth which is related to the actual material failure ahead of the crack tip. By means of FEM, the analysis of stress, strain and damage fields in a plate with a center crack is performed. The numerical simulation results of the fatigue crack growth are given and compared with the experimental ones.

2. EXPERIMENTS

2.1. *Material and specimen*

In this study, the material was 99.5% pure titanium in plate form. The chemical composition is given in Table 1. The geometry and dimensions of the crack propagation specimen are shown in Fig. 1. A circular hole of 2 mm in diameter was made at the center of the specimen to serve as a crack starter. All specimen were annealed under atmosphere at 540°C for 1 hour after machining. The surfaces of the specimens were polished with No. 2000 emery paper and alumina polishing suspension for microscopic observation.

2.2. *Experimental method and results*

The fatigue tests were performed in an electro-hydraulic servo-type fatigue testing machine (EHF-ED5TF-10L). The stress wave shape is sinusoidal, the stress ratio $r = 0$, the stress range is $\Delta\sigma = 80$MPa, and the stress frequencies are 2Hz, 6Hz, and 20Hz. The test temperature is 450°C. The growth of the fatigue crack was observed with a travelling microscope ($\times 50$). In order to obtain the related material parameters, the static tension tests at different strain rate were performed. Figure 2 shows the stress–strain curves under static tension. Figure 3 shows the relationship between the crack length l and the number of cycles N under different loading frequencies.

3. CONSTITUTIVE MODEL

The constitutive equations of the damaged material can be established by the CDM methods (Lemaitre and Chaboche, 1990; Lemaitre, 1992).

For virgin material, according to the general elasto/viscoplastic theory, we may take the visco plastic potential function Φ as:

$$\Phi = \frac{\gamma\kappa}{1+\alpha}\left(\frac{\sigma_{eq}}{\kappa} - 1\right)^{1+\gamma} \tag{1}$$

where, $\sigma_{eq} = (\frac{3}{2}\sigma'_{ij}\sigma'_{ij})^{1/2}$ is Mises equivalent stress, σ'_{ij} is deviatoric stress component, κ is hardening function, and α, γ are material constants depending on temperature.

Table 1. Chemical composition (wt%)

Fe	N	O	H	C
<0.047	<0.005	<0.098	<0.0021	<0.006

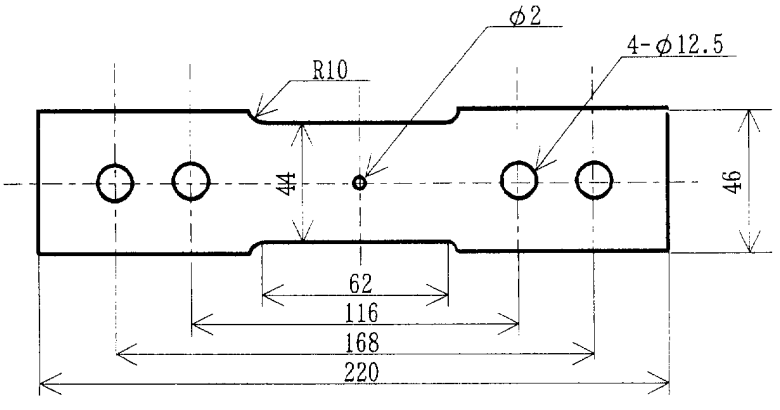

Fig. 1. The shape and size of fatigue specimen.

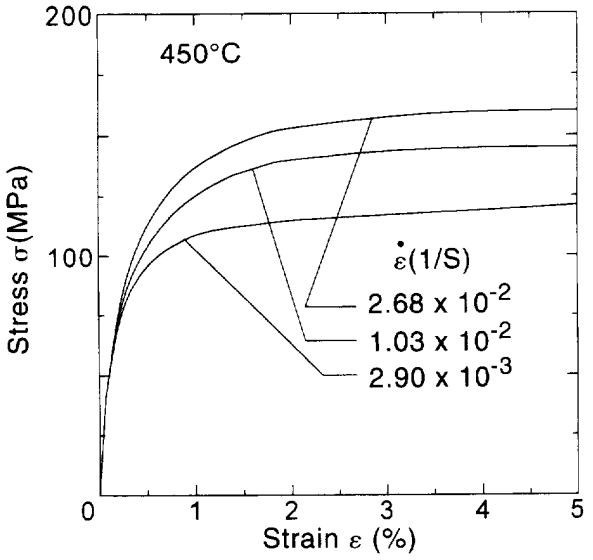

Fig. 2. The stress–strain curves in tension test.

From the normality hypothesis in actual stress space, this leads to:

$$\dot{\varepsilon}_{ij}^{vp} = \frac{3}{2}\gamma\left\langle \frac{\sigma_{eq}}{\kappa} - 1 \right\rangle^{n} \frac{\sigma'_{ij}}{\sigma_{eq}} \tag{2}$$

where, the symbol $\langle\ \rangle$ is defined as: $\langle x\rangle = 0,\ x \leqslant 0$; $\langle x\rangle = x,\ x > 0$.

For the damaged material, from the effective stress concept and the hypothesis of strain equivalence, the Cauchy stress tensor σ_{ij} is replaced by the damage effective stress tensor $\tilde{\sigma}_{ij}$

$$\tilde{\sigma}_{ij} = \frac{\sigma_{ij}}{1-D} \tag{3}$$

in the viscoplastic constitutive eqn (2). It follows,

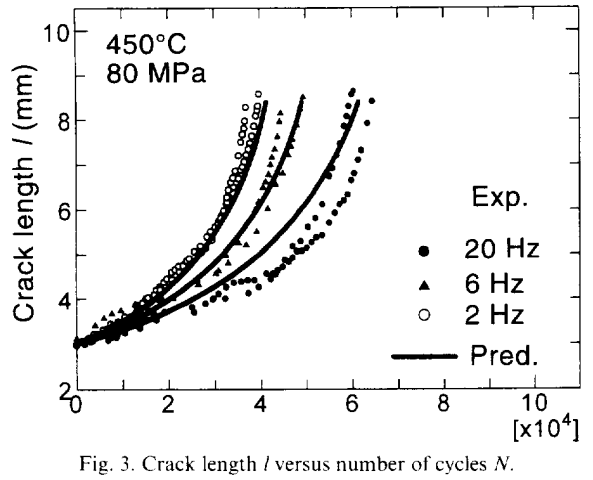

Fig. 3. Crack length l versus number of cycles N.

$$\dot{\varepsilon}_{ij}^{vp} = \frac{3}{2}\dot{\gamma}\left\langle \frac{\tilde{\sigma}_{eq}}{\kappa} - 1 \right\rangle^{\alpha} \frac{\sigma'_{ij}}{\sigma_{eq}} = \frac{3}{2}\dot{\gamma}\left\langle \frac{\sigma_{eq}}{\kappa(1-D)} - 1 \right\rangle^{\alpha} \frac{\sigma'_{ij}}{\sigma_{eq}}. \tag{4}$$

From the works of Murakami *et al.* (1986) and Chaboche (1988), the local damage evolution law may be assumed as,

$$\dot{D} = \begin{cases} C(\varepsilon_{eq}^{vp})^{\beta}\dot{\varepsilon}_{eq}^{vp} & \dot{\sigma}_{eq} > 0 \\ 0 & \dot{\sigma}_{eq} \leqslant 0 \end{cases} \tag{5}$$

where, for the sake of simplicity, we assume the damage is isotropic and is represented by a scalar. C and β are material parameters depending on temperature.

In the view of physics and material science, real engineering materials may have a crystalline structure that is made of a distribution of slip-planes or dislocations of different slip strength. So, it appears logical to conclude that the yield stress of the each slip-plane or grain is different. Based on the previous study (Takezono *et al.*, 1980; Takezono and Satoh, 1982; Sakamoto and Takezono, 1988) and micromechanics concepts (Lemaitre, 1990; Krajcinovic and Silva, 1982), a distribution fraction model may be established. In this model, it is assumed that the material consists of lots of elasto/perfectly-viscoplastic fractions, the yield stresses of fractions are different and are governed by some kind of distribution function. So, for the each fraction, its constitutive equation may be represented by eqns (2), (4) and (5).

As for the nonlocal macroscopic stress–strain relations, in accordance with the nonlocal concept (Bazant, 1991; Kachanov, 1992, Xia *et al.*, 1993), a nonlocal continuum formulation may be expressed as follows:

$$\mathrm{d}\sigma_{ij} = \int_0^{\infty} \psi(k_m)\,\mathrm{d}\sigma_{ij}^{m}\,\mathrm{d}k_m \tag{6}$$

$$\int_0^{\infty} \psi(k_m)\,\mathrm{d}k_m = 1 \tag{7}$$

$$\mathbf{D} = \int_0^{\infty} \psi(k_m) D(m)\,\mathrm{d}k_m \tag{8}$$

where, $\psi(k_m)$ is some kind of distribution function or weight function, k_m is the yield stress of mth fraction, $\mathrm{d}\sigma_{ij}^{m}$ is the stress increment tensor of mth fraction, $\mathbf{D}$ is nonlocal damage variable, and $D(m)$ is the damage variable of mth fraction.

To implement the formulation numerically, we may restrict the model to finite number fractions. So, the integral operations in eqns (6)–(8) are replaced by the summation operations as follows:

$$\Delta\sigma_{ij} = \sum_{m=1}^{n} \Delta\sigma_{ij}^{m} h_m \tag{9}$$

$$\sum_{m=1}^{n} h_m = 1 \tag{10}$$

$$\mathbf{D} = \sum_{m=1}^{n} D^{m} h_m \tag{11}$$

where n is the number of fractions, and its value can be any positive integer depending on the calculating accuracy and CPU time.

Table 2. Material parameters and related data at 450 C

m	1	2	3	4	5	6
α_m	6.0	5.0	5.0	2.0	2.0	1.0
γ_m(1/s)	2.0	4.0	8.0	16.0	24.0	32.0
h_m	0.3275	0.4175	0.1725	0.0544	0.0255	0.0026
k_m(MPa)	41	75	161	325	2302	3353

E = 62GPa, C = 0.04, β = 0.42 D_c = 0.60.

4. ANALYTICAL RESULTS AND DISCUSSION

The proposed model is incorporated into the finite element code. The related parameters are given in Table 2. α_m, γ_m, h_m, k_m, and E in this table are determined from the Fig. 2 by the same methods as Takezono and Satoh (1982) and Sakamoto and Takezono (1988). C, β and damage critical value D_c are determined by the fatigue experiment of smooth specimen (Qian *et al.*, 1995).

As an example, the finite element subdivision in the case of initial crack length l_0 = 2.0 mm is shown in Fig. 4a. The refined meshes near the crack tip are shown in Fig. 4b.

In the present study, according to the damage mechanics concepts, the fatigue crack growth behavior of material is controlled by the evolution and distribution of damage ahead of the crack tip. The crack advances to the next element when the average damage value (nonlocal) of the crack tip element reaches its critical value D_c.

The experimental results and the comparison between prediction and experimental results are shown in Fig. 3. From this figure, it is easy to see that the effect of loading frequency on the crack growth is remarkable. The numerical simulation has a good agreement with experimental ones.

Under the maximum load, the distributions of the maximum principal stress ahead of the crack tip at 6 different stages from initiation to fracture of the crack tip element are presented in Fig. 5. Here, N1–N6 represent the number of cycles at 6 different stages in an element fracturing process. The maximum principal stress coincides with the normal stress on the crack surfaces σ_y. From this figure, one may visualize that because there is no damage

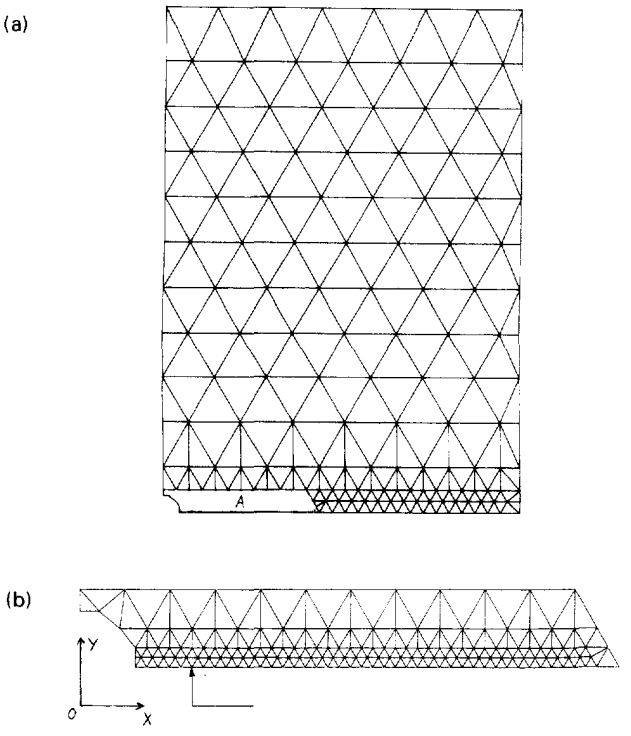

Fig. 4. (a) Finite element subdivision. (b) Details of A.

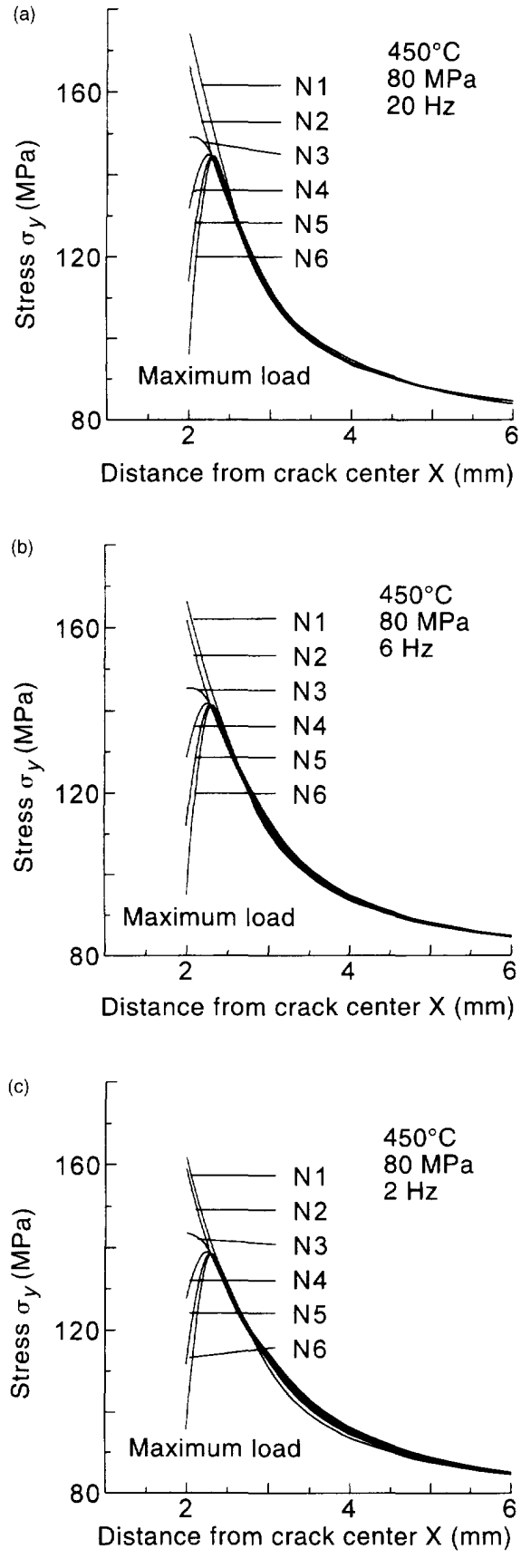

Fig. 5. Stress evolution during an element fracturing process: (a) 20 Hz, (b) 6 Hz, (c) 2 Hz.

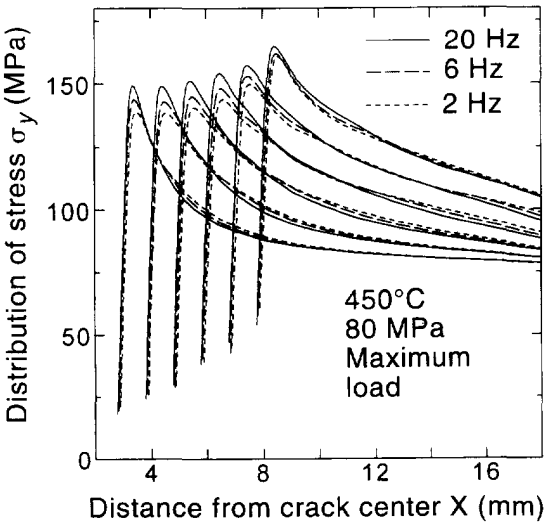

Fig. 6. Distributions of stress at different crack length.

in the material or the damage is so small that it can be neglected, at the cyclic initiation, such as N1, N2, the crack tip stress is the peak stress and the initial stress distribution shows a higher stress gradient near the crack tip, same as the distribution predicted by conventional FEM (no damage). With the increase of cyclic numbers, local damage and growth in the crack tip element occur, damaged material partly looses its loading capacity and local unloading takes place. So, the nonlocal (or total) stress in the crack tip element decreases rapidly. Obviously, this contradicts what the classical mechanics approach supposed that after an certain cycles, the stress field would reach a stable state which can be described by some conventional integrals, such as, J-integral, C*-integral, etc. This figure shows that no stable state of distribution stress is present at the crack tip element when damage in the material is taken into account.

Figure 6 shows the distributions of the maximum principal stress σ_y ahead of the crack tip at different crack growth stages. It is easy to see from the figure that the crack tip stress is lower than the peak stress and this peak stress takes place at a location away from the crack tip. It obviously contradicts what the classical parameters predict about the stress singularity at the crack tip, i.e. no stress singularity is present at the crack tip. It is interesting to note that peak stress becomes constant when crack length is in some region.

Figure 7 shows the distributions of the maximum principal viscoplastic strain ε_y^{vp} ahead of the crack tip at different crack growth stages. It is found from the figure that the viscoplastic strain is larger for lower loading frequency.

From above figures (Figs 5–7), it is easy to see that due to the effect of viscosity, the peak stress is lower, and the viscoplastic strain is larger, for lower loading frequency. Obviously, in the presence of material viscosity, loading frequency plays an important role.

The typical damage distributions at different crack lengths are shown in Fig. 8. It is found that in the fatigue crack growth process, the damage of material concentrates in a few elements near the crack tip, meaning that near the crack tip the material experiences serious damage. The value of accumulated damage near the crack tip is larger for lower loading frequency.

The stress–strain hysteresis loops at the crack tip element in the fatigue process ($l = 5$mm) are shown in Fig. 9. In this figure N1–N5 represent the number of cycles at 5 different stages in the crack tip element fracturing process. It is found that during the fatigue process, the loop width (i.e. viscoplastic strain range) becomes larger with the lower frequency. On the contrary, its height (i.e. stress range) becomes smaller.

Figure 10 shows that the crack growth rate is closely related to the viscoplastic strain range $\Delta\varepsilon_y^{vp}$ at the crack tip element. If dl/dN is plotted against $\Delta\varepsilon_y^{vp}$ in logarithmic coordinates, the relation follows a straight line and the data fall in narrow range regardless of the loading frequency.

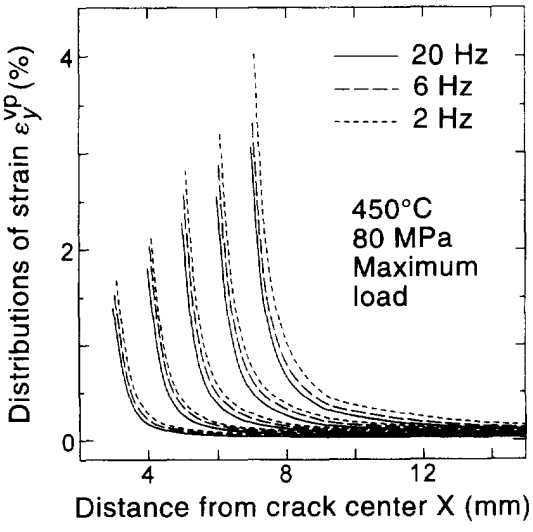

Fig. 7. Distributions of viscoplastic strain at different crack length.

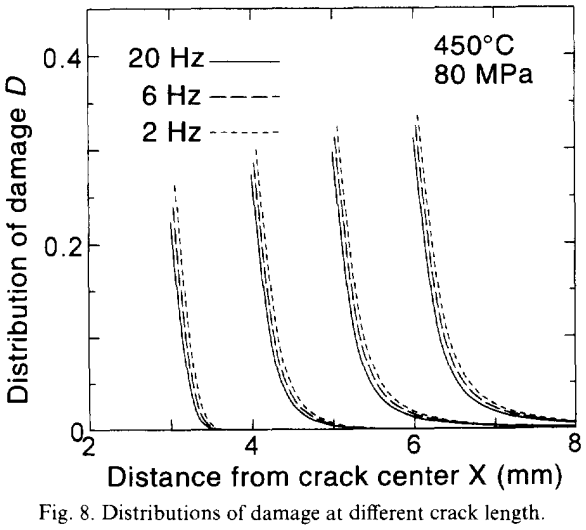

Fig. 8. Distributions of damage at different crack length.

5. CONCLUSIONS

Fatigue crack propagation tests of 99.5% pure titanium at 450°C for different loading frequencies were carried out. By means of FEM, the analysis of elasto/viscoplastic coupled with damage for the center crack growth specimen was performed. The mechanical fields (σ_{ij}, ε_{ij}, D) and the dependence of crack growth rate on frequency and viscoplastic strain at the crack tip were investigated in detail. The numerical results in the present study show that

(1) The stress at the crack tip element decreases rapidly with the cyclic numbers. There is no stable state of stress distribution ahead the crack tip in the fatigue process when material damage is taken into account.

(2) The crack tip stress is lower than the peak stress and the peak stress takes place at a location away from the crack tip. No stress singularity is present at the crack tip.

(3) In the presence of viscosity, the effect of loading frequency on the crack growth rate, stress, and viscoplastic strain of material is remarkable. The peak stress is lower and the viscoplastic strain is larger for lower loading frequency.

(4) The experimental fatigue crack growth rate $\mathrm{d}l/\mathrm{d}N$ is closely related to the $\Delta\varepsilon_y^{vp}$ obtained by numerical analysis. If $\mathrm{d}l/\mathrm{d}N$ is plotted against $\Delta\varepsilon_y^{vp}$, the relation can be expressed by a straight line in logarithmic coordinates for any loading frequency. So, the loading

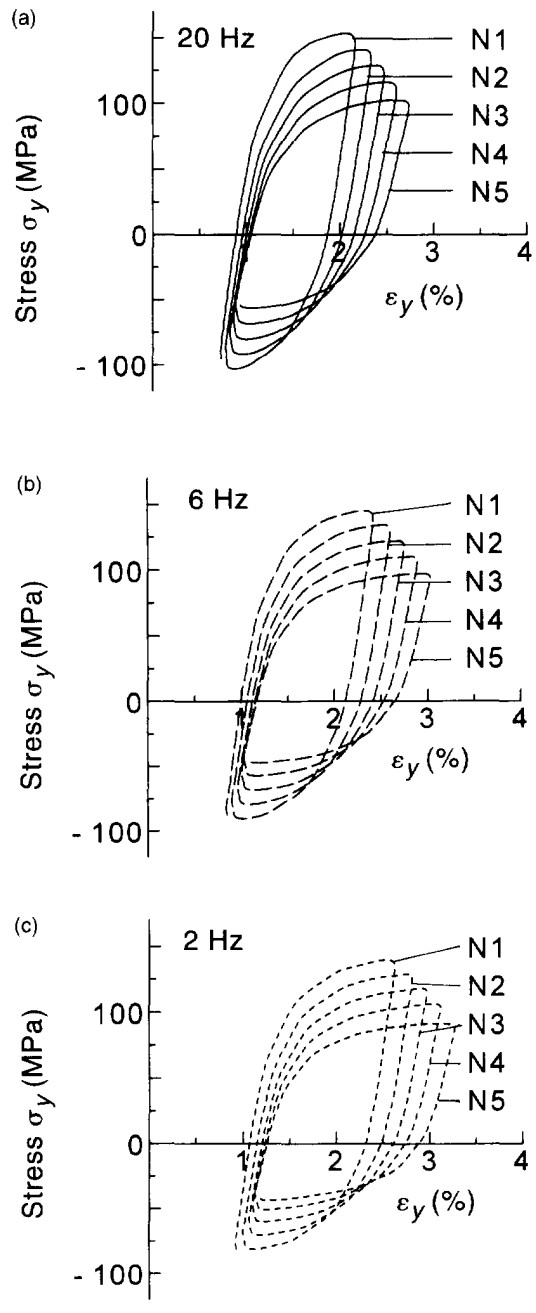

Fig. 9. Stress–strain hysteresis loops (crack length $l = 5$ mm): (a) 20 Hz, (b) 6 Hz, (c) 2 Hz.

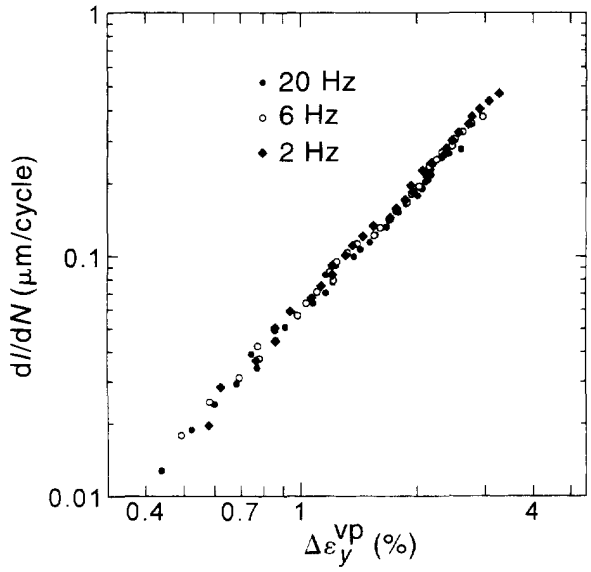

Fig. 10. Relations between dl/dN and $\Delta\varepsilon_y^{vp}$.

frequency dependence of crack growth may be explained by the strain rate dependence of material.

Acknowledgements— The study was supported by a fellowship to the first author from the Japanese Ministry on Education, Science and Culture.

REFERENCES

Bazant, Z. P. (1991). Why continuum damage is nonlocal: micromechanics arguments. *J. Engng Mech., ASCE* **117**(5), 1070–1087.

Chaboche, J. L. (1988). Continuum damage mechanics: Part I—General concepts. Part II—Damage growth, crack initiation, and crack growth. *ASME. J. Appl. Mech.* **55**, 59–72.

Chaboche, J. L. and Bathias, C. (1986). On the creep crack growth prediction by a local approach. *Engng Fract. Mech.* **25**, 677–691.

Chen, G. G. and Hsu, T. R. (1991). Effects of cyclic plasticity on creep crack growth. *Engng Fract. Mech.* **39**, 509–524.

Kachanov, M. (1992). Effective elastic properties of cracked solids. *Appl. Mech. Rev.* **45**(8), 304–335.

Krajcinovic, D. and Silva, M. A. G. (1982). Statistical aspects of the continuous damage theory. *Int. J. Solids Structures* **18**, 551–562.

Lemaitre, J. (1992). *A Course on Damage Mechanics*. Springer-Verlag, Germany.

Lemaitre, J. (1990). Micro-mechanics of crack initiation. *Int. J. Fracture* **42**, 87–99.

Lemaitre, J. and Chaboche, J. L. (1990). *Mechanics of Solids Materials*. Cambridge University Press, Cambridge.

Murakami, S., Sanomura, Y. and Hattori, M. (1986). Modelling of the coupled effect of plastic damage and creep damage in Nimonic 80A. *Int. J. Solids Structures* **22**, 373–386.

Qian, Z. X., Takezono, S., and Tao, K. (1995). A damage mechanics approach to high temperature fatigue crack growth. In *Fatigue and Crack Growth: Enviromental Effects, Modeling Studies, and Design Considerations*. ASME 1995, PVP-Vol. 306, 317–322.

Sakamoto, H. and Takezono, S. (1988). Fatigue crack propagation under step variation of stress frequency in orthotropic material. *Engng Fract. Mech.* **31**, 463–474.

Takezono, S. and Satoh, M. (1982). Effect of stress frequency on fatigue crack propagation in titanium. *ASME J. Engng Mater. Technol.* **104**, 257–261.

Takezono, S., Tao, K. and Kanezaki, K. (1980). Elasto-visco plastic dynamic response of axisymmetrical shells by overlay model. *ASME. J. Pressure Vessel Technol.* **102**, 257.

Xia, S., Takezono, S. and Tao, K. (1993). Nonlocal elastic damage near crack tip. *Int. J. Fracture* **62**, 87–95.